DOI: 10.24427/978-83-67185-30-1_35

Multiple inlet micro pin fin heat sink for heat transfer performance improvement

Paweł DĄBROWSKI[(a)], Ritunesh KUMAR[(b)], Dariusz MIKIELEWICZ[a)], Vikas YADAV[(b)]

[(a)] Gdańsk University of Technology, Narutowicza 11/12, 80-233 Gdańsk, Poland
[(b)] Indian Institute of Technology, Indore, India
ritunesh@iiti.ac.in

ABSTRACT

A detailed numerical study has been prepared to analyze a new design of a multiple inlet/outlet micro pin fin heat sink (MPFHS) and to compare its effectiveness in heat spreading with a conventional design based on the single inlet and single outlet configuration. The new design contains 4 manifolds placed on the sides of the heat sink. Moreover, the inlet channels have been shifted to the corners of the manifolds to create a vortex inside the heat sink and to reduce the maximum temperature of the heat sink's surface. The aim of the study is to find the best design of the multiple inlet/outlet MPFHS in terms of thermohydraulic performance and the most uniform temperature profile. Besides, the other 2 designs have been tested: multiple inlet and multiple outlet designs without vortex generator. During the study, water and copper have been assumed as fluid and solid domains respectively. The heat flux assumed to be dissipated by the heat sink was equal to 150 W/cm2. The maximum, average, and minimum temperatures of the fluid and solid domain have been compared for various cases as well as pressure drops, velocity profiles, and streamlines. Moreover, parameters that allow describing particular cases in terms of temperature uniformity and heat transfer performance, namely mean absolute temperature difference, thermal resistance, Nusselt number, and overall thermal performance factor have been calculated. To get the most reliable comparison between particular cases, the same amount of fluid flowing in the MPFHS for all cases has been assumed. The results show that the multiple inlet with vortex generator design is characterized by the best thermohydraulic performance. The maximum temperature, mean average temperature difference, and thermal resistance can be reduced by 21.1%, 61.3%, and 23.5% respectively.

Keywords: computational fluid dynamics; vortex, flow distribution, maldistribution, heat transfer intensification.

1. INTRODUCTION

The electronic devices need to operate below some temperature level at which they are designed to ensure their reliability and long-term service life. Those levels depend on the application and manufacturer. However, there are some broadly accepted ranges of temperature that a particular electronic device should not exceed (Cactus Technologies, 2021):

- from 0°C to 70°C for commercial applications,
- from -40°C to 85°C for industrial applications,
- from -55°C to 125°C for military applications.

The small size and high density of ICs in electronic devices make the thermal management of these devices challenging and complex. Tuckerman and Pease (1981) suggested the use of water cooled microchannel heat sink (MCHS) for electronic cooling. Small size, light weight, high heat transfer coefficient, and large heat transfer surface area are some of the qualities of MCHS which make them apposite for various applications like rocket engines, avionics, hybrid vehicle power electronics, turbine blades and refrigeration systems (Mudawar, 2011). MCHS even projected as twenty first century cooling solution (Kadam, Kumar, 2014). The demand to make MCHS more efficient in thermal management is continuously increasing since it was first introduced in 1981. Researchers have explored and proposed various techniques/designs for heat transfer augumentation through MCHS. Some of the promising

techniques are flow disruptions (Xu et al., 2016; Wang et al., 2015), surface roughness (Shokouhmand et al., 2009), channel curvature (Gong et al., 2011; Mohammed, 2011), re-entrant obstructions (Chai et al., 2013), secondary flows (Lee et al., 2013; Ghani et al., 2017), double layered (Hung et al., 2012), fluid additives (Jang et al., 2006; Ho et al., 2009; Hung et al., 2012b) and micro pin fins (Yadav et al., 2015).
High heat transfer coefficient, simple and inexpensive structure of pin fins make them suitable for extensive applications. Peles et al. (2005) in their research able to achieve low wall temperatures while dissipating high heat fluxes using bank of micro pin fins. Qu and Siu-Ho (2008) analyzed heat transfer characteristics with array of staggered micro pin fins of square shape having equivalent diameter 200 μm and height 670 μm. Water as coolant having Reynolds number ranging from 45.9 to 179.6 at two inlet temperatures (30°C and 60°C) was used. They proposed two correlations of Nusselt number with the help of their results. Rubio-Jimenez et al. (2012) proposed MPFHS based on concept of increasing heat transfer area as coolant temperature increases. This novel variable-density fin heat sink able to maintain overall temperature gradient lower than 2 K/mm. Their best heat sink configuration has thermal resistance ranges from 0.14 to 0.25 K/W.
Even though above mentioned design changes improves heat transfer performance of MCHS still all these heat sinks including MPFHS suffers from flow maldistribution problem (Dąbrowski, 2020) with needs to be addressed, to further improve the performance and long life of electronic device. Flow maldistribution in heat sink largely depends on the way fluid enters the heat sink. Researchers have suggested various inlet/outlet configurations and plenum designs to mitigate flow maldistribution in heat sinks (Chein and Chen, 2009; Sehgal et al., 2011; Pattamatta and Das, 2014; Xia et al, 2015). Yadav et al. (2019) proposed new technique of splitting inlet port into two separate inlet ports to mitigate flow maldistribution in conventional MCHS. Different configurations of front inlet and side inlet designs are compared to their conventional designs. Their best designs reduce flow misdistribution about 26.2% in case of front inlet and 68.5% in case of side inlet when compared to their respective conventional designs. Kumar et al. (2018) proposed the new approach of microchannels having variable width. Their design reduces flow maldistribution up to 93.7% which is able to reduce temperature fluctuation at solid-fluid interface by 4.3 K. Recently Kumar et al. (2020) proposed a new fluid flow distribution scheme to mitigate surface temperature non-uniformity in MPFHS which is the critical issue in modern microprocessors chip cooling. They proposed two front facing multi-inlet designs ($MPFHS_{MI,F}$ and $MPFHS_{MI,FH}$) and one side facing multi-inlet design ($MPFHS_{MI,SH}$). Their designs able to reduce surface temperature non-uniformity by 7.6 K ($MPFHS_{MI,F}$), 24 K (MPFHSMI,FH), 7.4 K ($MPFHSM_{I,SH}$) as compared to conventional design. These design average Nusselt number also 26.7% ($MPFHS_{MI,F}$), 52.3% ($MPFHS_{MI,FH}$) and 70.9% (MPFHSMI,SH) higher than conventional design of MPFHS. In search of more efficient fluid flow distribution in MPFHS, the current paper proposed novel MPFHS designs having 4 side manifolds instead of 2 (as in conventional designs) and one manifold on the top of heat sink. The results of thermohydraulic performance are compared with conventional MPFHS.

2. CFD MODEL DETAILS

Before starting the numerical simulation, the micro pin fin heat sinks (MPFHS) with various inlet/outlet configurations have been designed. Three-dimensional models were created with the ANSYS SpaceClaim software and then the discretized fluid and solid domains were prepared. The working fluid was assumed as water and a heat sink material was copper.
The solid domain of MPFHS with all dimensions has been presented in Figure 1. The heat flux was applied to the bottom surface in the Z-axis direction. The fluid domain where the water flows through the MPFHS has been created based on the solid domain – the height of the fluid domain is equal to the height of pin fins (0.4 mm). The MPFHS needs manifolds that distribute and collect fluid from the inlet to the outlet. The manifolds used in this study have been shown in Figure 2. The inlet and outlet configuration is changing for various cases. The side manifolds in the amount of 2 or 4 (depending on the particular case) were placed on the side edges of the MPFHS, while the top manifold was placed at the center of the upper area of the MPFHS. The hydraulic diameter Dh of the inlet/outlet channel in the side manifold is equal to 640 μm and in the top manifold 1 600 μm. The total areas of inlet channels and outlet channels for every case are always the same and equal to 2.56 mm2. Moreover, the hydraulic diameter of channels created by the pins is equal to 308 μm.

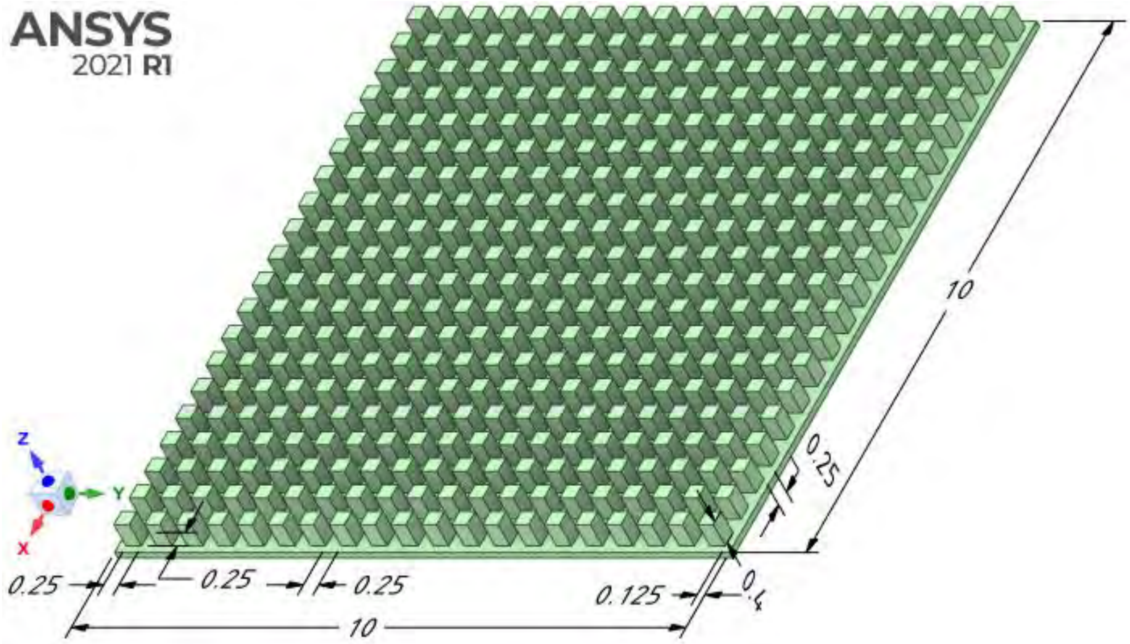

Figure 1: The solid domain (copper) with 400 micro pin fins

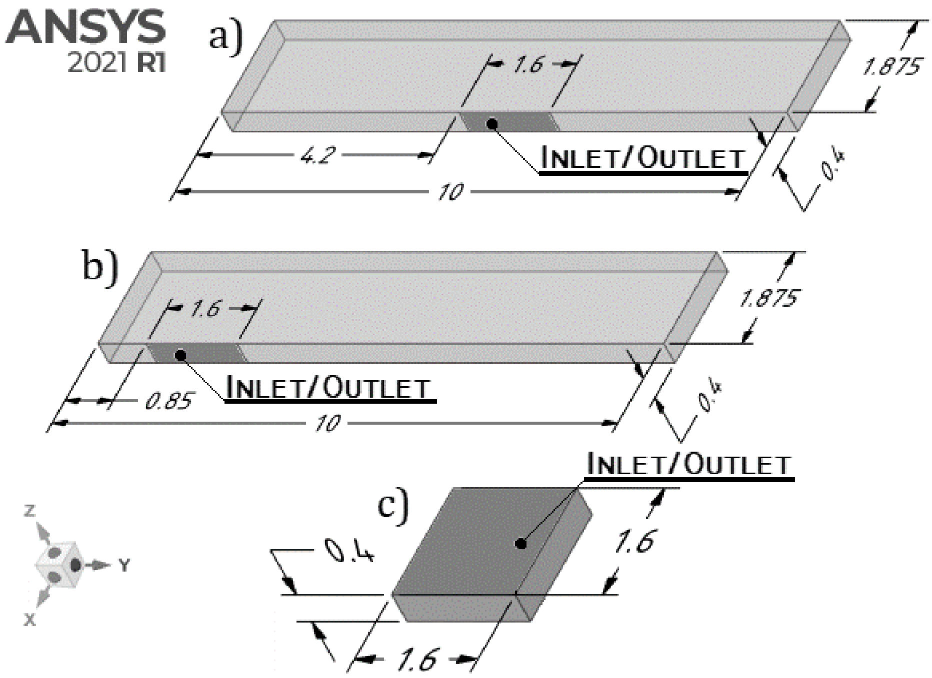

Figure 2: The fluid domains (water) of manifolds: a) side manifold without vortex configuration; b) side manifold with vortex configuration; c) top manifold

In the current study, 4 various cases with different inlet/outlet configurations are tested and compared. Case 0 is a conventional case with 1 inlet and 1 outlet, both on the side manifolds. Case 1 is a multiple outlet case with 1 inlet and 4 outlets, where the inlet is on the top manifold and the outlets are on the side manifolds. The model of Case 2 is the same as for Case 1 but there is a difference between inlets and outlets. Case 2 is a multiple inlet case with 4 inlets and 1 outlet, where inlets are on the side manifolds and the outlet is on the top manifold. Case 3 is similar to Case 2, so it has 4 inlets on the side manifolds and 1 outlet on the top manifold. However, the inlets on the side manifolds were shifted to the corners to create a vortex configuration.

During the investigation following assumptions were taken:

- The physical properties of fluid were constant.
- Fluid flow was a single-phase, steady-state, incompressible, and three-dimensional.
- Radiation heat transfer from surfaces was neglected.
- The effect of gravity was neglected.

The continuity, momentum, and energy equations (Eq. (1), Eq. (2), and Eq. (3)) were taken into account as governing equations and used in calculations together with the above-mentioned assumptions. Moreover, the energy balance equation inside the solid domain (Eq. (4)) was used.

$$\nabla \cdot \vec{V} = 0 \qquad \text{Eq. (1)}$$

$$\rho(\vec{V} \cdot \nabla \vec{V}) = -\nabla p + \mu \nabla^2 V \qquad \text{Eq. (2)}$$

$$\rho C_p (\vec{V} \cdot \nabla T) = k_f \nabla^2 T \qquad \text{Eq. (3)}$$

$$k_s \nabla^2 T = 0 \qquad \text{Eq. (4)}$$

In ANSYS FLUENT 2021 R1 the above-mentioned equations are solved using the finite volume method (FVM). The momentum equation was discretized by the second-order upwind scheme. The realizable k-epsilon model with enhanced wall treatment has been chosen as a turbulence model. Other models have been also tested, but the above-mentioned gives the best convergence. Moreover, the SIMPLE scheme has been chosen to couple pressure and velocity in the whole section.
Water was chosen as a working fluid for all the considered cases. The inlet parameters for water are ρ=998.2 kg/m3, μ=1.003e-3 Pa s, Cp=4182 J/(kg·K), kf=0.6 W/(m·K) and T=288.15 K and the parameters for copper are ρ=8978 kg/m3, Cp=381 J/(kg·K), ks=387.6 W/(m·K). The heat was applied at the bottom wall of a section with a constant value of heat flux q of 150 W/cm2. The constant mass flow rate boundary condition was assumed at the inlet to the heat sink. The pressure-outlet (gauge pressure of 0 Pa) boundary condition was assumed at the outlet of the heat sink. When the residual values become less than 10-3 for the continuity, x-velocity, y-velocity, and z-velocity and 10-6 for the energy the solutions are considered to be converged. The inlet, outlet, and pin fins parameters for various cases have been shown in Table 1. The parameters were set in such a way to ensure the constant mass flow rate for the entire heat sink but then Reynolds numbers and mass fluxes in pin fins are not equal in the conventional and novel designs.

Table 1. Inlet and outlet parameters for various cases tested

	Case 0	**Case 1'**	**Case 2'**	**Case 3'**
$\dot{m}_{in}$ [kg/s]	1.50e-3	1.50e-3	3.75e-4	3.75e-4
Re_{in} [-]	1 496	935	374	374
G_{in} [kg/m^{2}s]	2 344	586	586	586
$\dot{m}_{out}$ [kg/s]	1.5e-3	3.75e-4	1.5e-3	1.5e-3
Re_{out} [-]	1 496	374	935	935
G_{out} [kg/m^{2}s]	2 344	586	586	586
Re_{pin} [-]	230	58	58	58
G_{pin} [kg/m^{2}s]	750	187.5	187.5	187.5

3. MODEL VALIDATION

The mesh independence study was carried out to ensure the accuracy of numerical results. There were four different mesh types tested: Coarse (3.9e6 elements), Medium (5.8e6 elements), Fine (1.1e7 elements) and Very Fine (1.8e7 elements). To compare various meshes, the percentage deviation ε of tested parameter F (velocity, pressure drop, temperature) between the j-th mesh and the Very Fine mesh has been introduced (Eq. (5)). The mesh for which the absolute percentage deviation is less than 1% for maximum fluid velocity, total pressure drop and the maximum temperature in fluid and solid domains has been chosen for all simulations. Mesh independence study has been prepared for the following boundary conditions: Case 2', inlet mass flow rate of 3.75e-4 kg/s, an inlet temperature of 288.15 K, and heat flux of 150 W/cm2 at the bottom wall. The Fine mesh (1.0e7 and 1.1e7 elements for Case 0 and the rest of the cases respectively), has been chosen for further calculations.

$$\varepsilon = \left| \frac{F_j - F_{v.fine}}{F_{v.fine}} \right| \times 100\% \quad \text{Eq. (5)}$$

4. RESULTS AND DISCUSSION

To compare various cases to each other, several variables (Nusselt number, mean average temperature difference, thermal resistance, and overall thermal performance factor) have been introduced.

The Nusselt number describes how much the convective heat transfer is larger than the conductive heat transfer (Cengel and Ghajar, 2015). In the current study, the average value has been used, according to Eq. (6). The higher the Nusselt number, the more intense convective heat transfer, which is very favorable for heat sink design.

$$Nu = \frac{qD_h}{k_f (T_{avg,s} - T_{avg,f})} \quad \text{Eq. (6)}$$

The mean average temperature difference δ (Pham-gia and Hung, 2001; Wang et al., 2022) has been introduced in Eq. (7) to compare the cases to each other in the scope of temperature uniformity. The lower the δ is, the more uniform the temperature profile for the particular case is.

$$\delta = \frac{\left| T_{\max} - T_{avg} \right| + \left| T_{\min} - T_{avg} \right|}{2} \quad \text{Eq. (7)}$$

The parameter that quantitatively defines the heat sink's capability of heat spreading is the total thermal resistance R presented in Eq. (8). The R reflects the heat transfer capacity of the particular case.

$$R = \frac{T_{\max,s} - T_{in,f}}{qA} \quad \text{Eq. (8)}$$

During the heat transfer intensification it is very common that with the increase of Nusselt number (effect), the pressure drop (cost) is also increased. The non-dimensional parameter that takes into account both cost and effect has been proposed by Yadav et al. and shown in Eq. (9).

$$\eta_i = \frac{Nu_i / Nu_{ref}}{(\Delta p_i / \Delta p_{ref})^{1/3}} \quad \text{Eq. (9)}$$

The minimum, average and maximum temperatures for solid and fluid domains have been analyzed for various cases and have been shown in Figure 3. As can be seen, the maximum temperature of the heat sink for the conventional case (Case 0) is above 80°C, which is too high value for commercial application electronic devices. The maximum temperature of the solid is equal to 125.8 K when 4 outlets are introduced (Case 1') and it is even slightly too high for military applications. However, the maximum temperature of the solid can be reduced by 3.5 K compared to the conventional case when 4 inlets are introduced (Case 2') but in Case 2' the average and minimum temperatures are much higher. It means that the temperature profiles look much different in Case 1' and Case 2'. A significant reduction of maximum temperature can be observed for Case 3', so the 4 inlets with vortex generator case. Here, the maximum temperature is below 67°C so in the range of commercial application electronic devices. The maximum temperature has been reduced by 18.0% compared to the conventional case. Moreover, the differences between maximum, average, and minimum temperatures are small compared to Case 0, which means that using the vortex generator design for the heat sink cooling results in a much more uniform temperature profile.

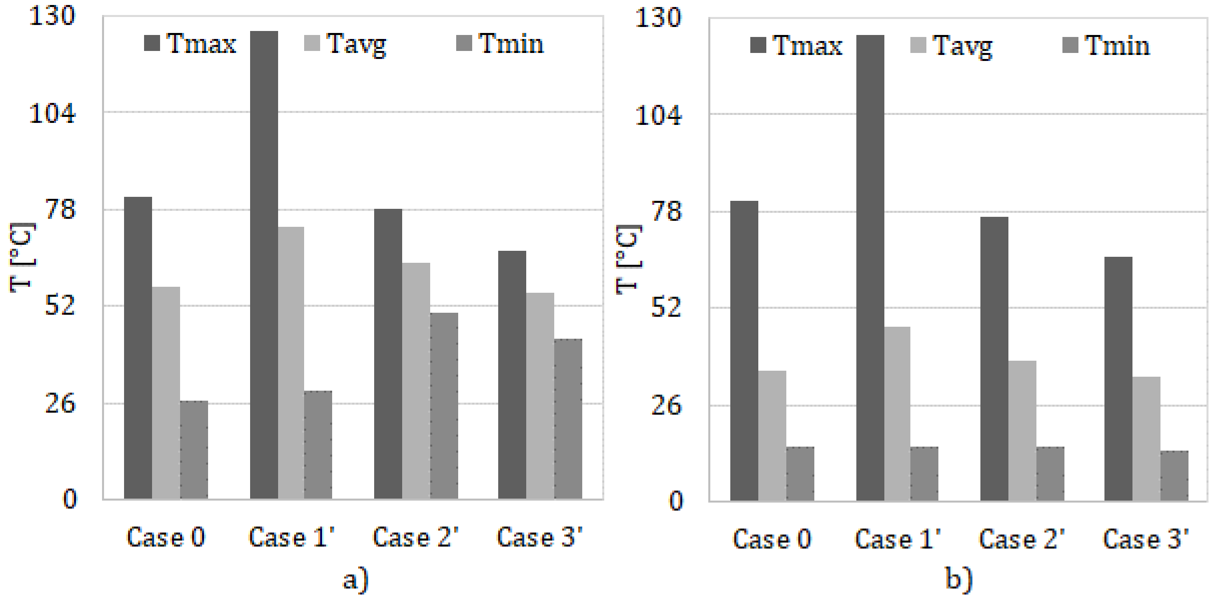

Figure 3: Maximum, average, and minimum temperature for various cases: a) solid domain; b) fluid domain

In current studies, the pressure-outlet with a gauge pressure of 0 Pa boundary condition has been assumed, so the pressure drop is equal to the inlet pressure for the particular case. Both Case 0 and Case 1' have one inlet, while Case 2' and Case 3' have four inlets. However, it is assumed that those inlets are fed in series so the total pressure drop is the average of all pressures at the inlets. The pressure differences between particular inlets in multiple inlet cases were negligible. The next thing that should be taken into account during designing a heat sink is thermal resistance, which presents how much temperature difference between the cooling fluid and the heat sink's wall is needed to transfer the unit of heat during the unit of time. The lower the value is, the better, in terms of heat transfer, the heat sink is.

Both resistances for various cases are shown in Figure 4. The smallest pressure drop occurs for Case 1', namely 3.1 kPa, and the highest for Case 0, namely 8.5 kPa. It is connected with the assumption that the total area of the inlet channels and outlet channel is the same. Hence, the inlet channel area in Case 1' (1 inlet and 4 outlets) is 4-times higher than the inlet area in the conventional case (1 inlet and 1 outlet), so the pressure drop for the same inlet mass flow rate is lower. Even for the jet impingement flow, which occurs in Case 1' when the inlet is placed at the top of the heat sink and the working medium is entering the manifold perpendicular to the heat sink's surface. The remaining 2 cases with multiple inlet, namely Case 2' and Case 3' show increased pressure drop, compared to Case 1' but not significant. The pressure drop for Case 2' and Case 3' is 3.2 kPa and 3.4 kPa respectively, which is a reduction of 62.4% and 60.0% respectively compared to the conventional case.

In Figure 4b the thermal resistance for various cases is shown. Case 1' is characterized by the highest thermal resistance among the analyzed cases and is equal to 0.28 K/W, while the conventional case's thermal resistance is 0.17 K/W. As mentioned earlier, due to a very non-uniform temperature profile, Case 1' is not showing thermal advantages. However, Case 2' is promising with a thermal resistance of 0.16 K/W, which is a 5.9% of reduction. Moreover, using the vortex generator design (Case 3'), the thermal resistance can be reduced by 23.5% (compared to Case 0), namely to 0.13 K/W.

The very important thing during a heat sink design is to assure the uniform fluid flow over the heat sink's surface and as an effect, the uniform temperature profile. The non-uniform temperature results in occurring of hotspots which can provide local boiling or even dryout of the cooling medium. Both are undesirable phenomena (if single-phase flow has been assumed) that can easily damage the electronic device.

The next parameter which describes quantitatively, whether individual cases are better than conventional design or not, is the overall thermal performance factor η. The conventional design is the baseline, so η for Case 0 is equal to 1.0. If the value of η for a particular case is higher than

1.0, the case can be considered better than the conventional design. If the value of η is lower than 1, it is the opposite.
Both thermal parameters that quantitatively describe the heat sink performance for various cases have been presented in Figure 5.

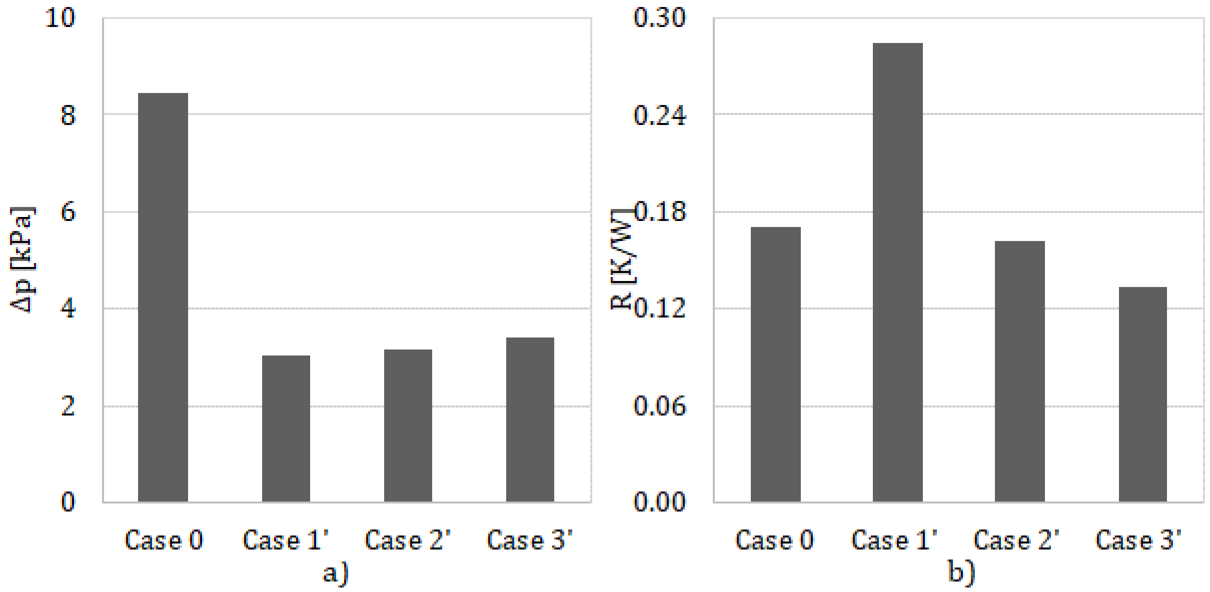

Figure 4: Resistances for various cases: a) total hydraulic resistance; b) total thermal resistance

The mean average temperature difference δ (Figure 5a) for the conventional case is equal to 27.4 K and 33.0 K for solid and fluid domains respectively. Providing fluid at the top of the heat sink with 4 outlet manifolds at the sides (Case 1') significantly increases (by 76.3% and 67.3%) δ for the solid and fluid domains respectively. Hence, Case 1' is not promising in terms of uniform fluid distribution. However, Case 2' is much more promising because the reduction of δ, compared to Case 0, is significant. The reduction of δ for a solid domain is 49.3% while 6.4% for a fluid domain. An even higher reduction can be obtained when 4 inlets are shifted to the corners of the manifolds (Case 3'), namely 56.9% and 20.6% for solid and fluid domains respectively. In the vortex generator design, the mean average temperature difference δ is 11.8 K for the solid domain and 26.2 K for the fluid domain.
The overall thermal performance factor η analysis is shown in Figure 5b. Each case shows thermal performance improvement compared to the conventional case. In the current comparison approach, the Nusselt number is smaller than for Case 0, which is equal to 35.5. For novel designs, the Nusselt number is 17.7%, 16.6, and 1.4% smaller, namely equal to 29.2, 29.6, and 35.0 for Case 1', Case 2', and Case 3' respectively. Due to the constant mass flow rate for the entire heat sink (4-times lower in the side manifolds), the Reynolds number in the pin fins is also 4-times smaller than for the conventional case (Table 1). As is known (He et al., 2020) the higher the Reynolds number, the higher the Nusselt number is. Hence, the 1.4% reduction of the Nusselt number for Case 3' connected with a significant reduction of Reynolds number can be considered a good result. Nevertheless, the overall thermal performance factor η is still higher than 1.0 and equal to 1.15, 1.16, and 1.33 for Case 1', Case 2', and Case 3' respectively because the pressure drop is reduced in the novel designs.
To get a broader view of the hydrodynamic behavior in the particular designs of micro pin fin heat sinks, the streamlines colored by velocity magnitude have been generated. The streamlines in the MPFHS with local velocity scales have been presented in Figure 6. It can be seen that in the conventional case (Case 0) most of the flow is realized in the center of the heat sink due to I-type flow configuration, which is connected to a flow maldistribution phenomenon and in effect generates non-uniform temperature profile. Case 1' is characterized by the jet impingement flow at the center of the MPFHS where the velocity is the highest. The working fluid flows from the center of the heat sink mostly straight to the outlet manifolds, resulting in non-uniform distribution and a small amount of fluid in the corners of the MPFHS. It is, as in the previous case, connected with the I-type flow configuration. Introducing 4 inlets on the side of the MPFHS (Case 2') results in a more uniform flow. The fluid spreading

in the wider area of the MPFHS entrance and only small surfaces at the corners are lacking the flow. To overcome this issue, Case 3’ has been proposed where inlets have been shifted to the corners, generating a vortex in the MPFHS. In this case, almost the entire heat sink surface is fed with the working fluid and the flow maldistribution is low which influences the temperature field positively. There is still a room in Case 3’ for optimization of the inlets positions to obtain as uniform flow as possible. It is described in the further subsection.

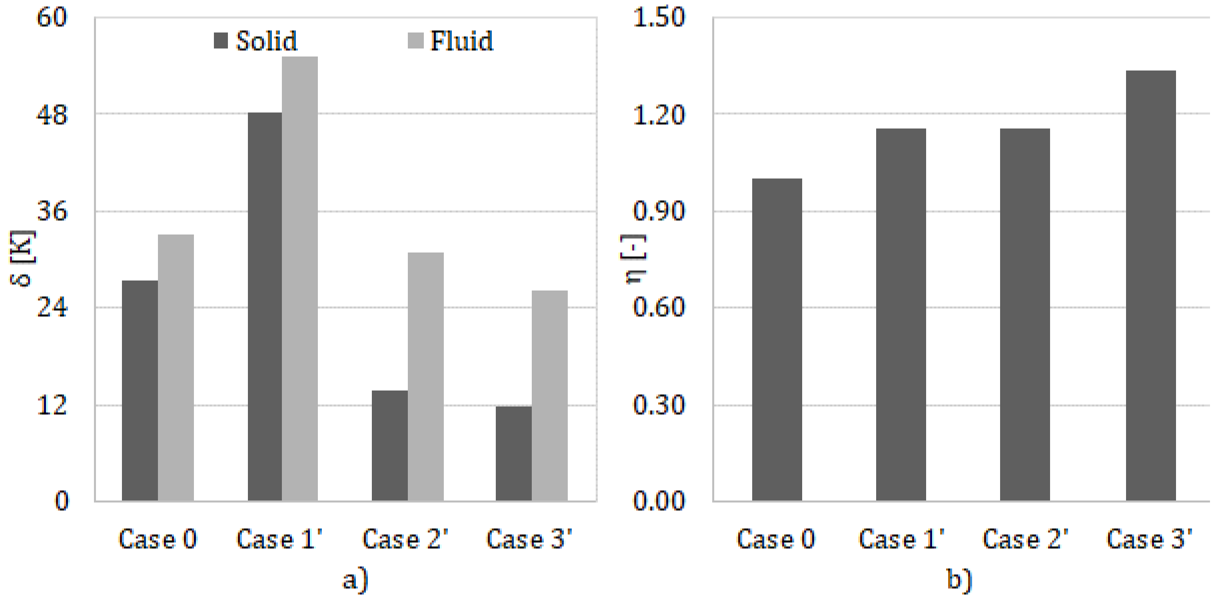

Figure 5: Thermal parameters for various cases: a) mean average temperature difference for solid and fluid domains; b) overall thermal performance factor

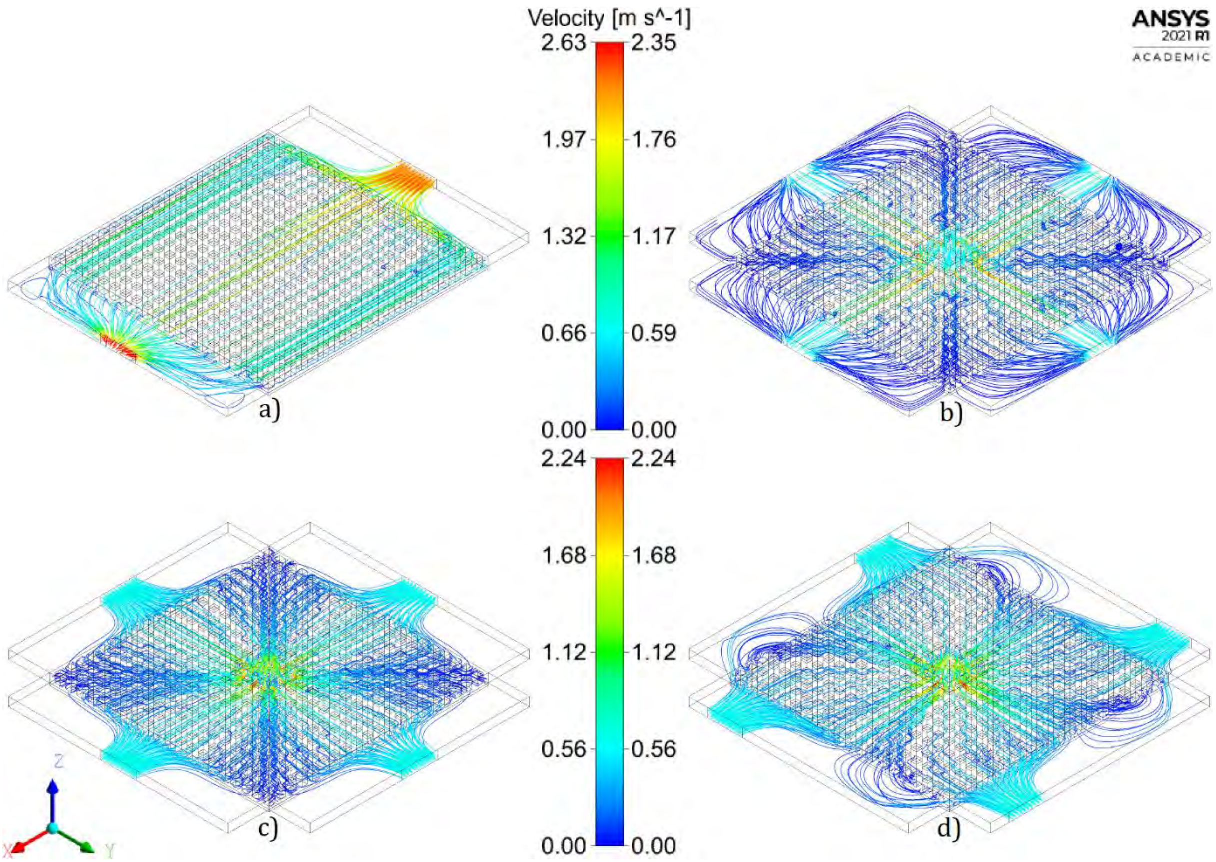

Figure 6: Streamlines from inlet to outlet colored by velocity magnitude - local scale: a) Case 0; b) Case 1’; c) Case 2’; d) Case 3’

The temperature fields in the MPFHS for various cases with local scale have been presented in Figure 7. For Case 0 the temperature field is very non-uniform. Due to the I-type flow configuration, where most of the working medium flows in the center of the MPFHS, the temperature is low in the center but high on both sides of the MPFHS. The maximum solid temperature for Case 0 is equal to 81.5°C and is placed in the corners near the outlet manifold. This case with such thermohydraulic parameters is not suitable for commercial applications of electronics cooling. The temperature field for Case 1' is much different from Case 0. The single inlet at the top of MPFHS and jet impingement flow results in temperature reduction only in the center part of the heat sink. However, due to the direct flow to the outlet channels, which are located in a straight line from the center, the corners of MPFHS suffer from high temperatures. Overall, the maximum temperature is increased by 54.2% compared to Case 0. When 4 inlets are placed at the sides of the heat sink (Case 2') the temperature field is much more uniform than for Case 0 and Case 1'. The reduction of maximum temperature compared to Case 0 is 4.3%, so it is not significant but, as described previously, the temperature uniformity is much larger. It is worth noticing, that the minimum temperature is 87.7% higher than the minimum temperature in Case 0. It is connected with the fact that in Case 2' the inlet mass flow rate is 4-times lower than in Case 0 but in total, mass flow rates for the entire heat sink are the same (4 inlets in Case 2'). Hence, the mass flow rates on MPFHS near the inlets in Case 2' are relatively low compared to the mass flow rate on MPFHS near the inlet in Case 0. Low mass flow rate results in high temperature. However, looking at the heat sink as a whole, the mass flow rate is the same in every case (mass fluxes for pins are the same) and the maximum temperature can be reduced thanks to uniform fluid distribution which is the most important thing. After shifting inlet channels to the corners of MPFHS (Case 3'), the temperature field is even more uniform and a significant maximum temperature reduction can be observed. The vortex case can be utilized in the commercial applications of electronics cooling because the temperature peak is lower than 70°C. The maximum temperature is reduced by 18.0% compared to Case 0. The minimum temperature is higher, as in Case 2' but the increase is lower, namely 61.6%. The explanation for so high minimum temperature is the same as for Case 2'.

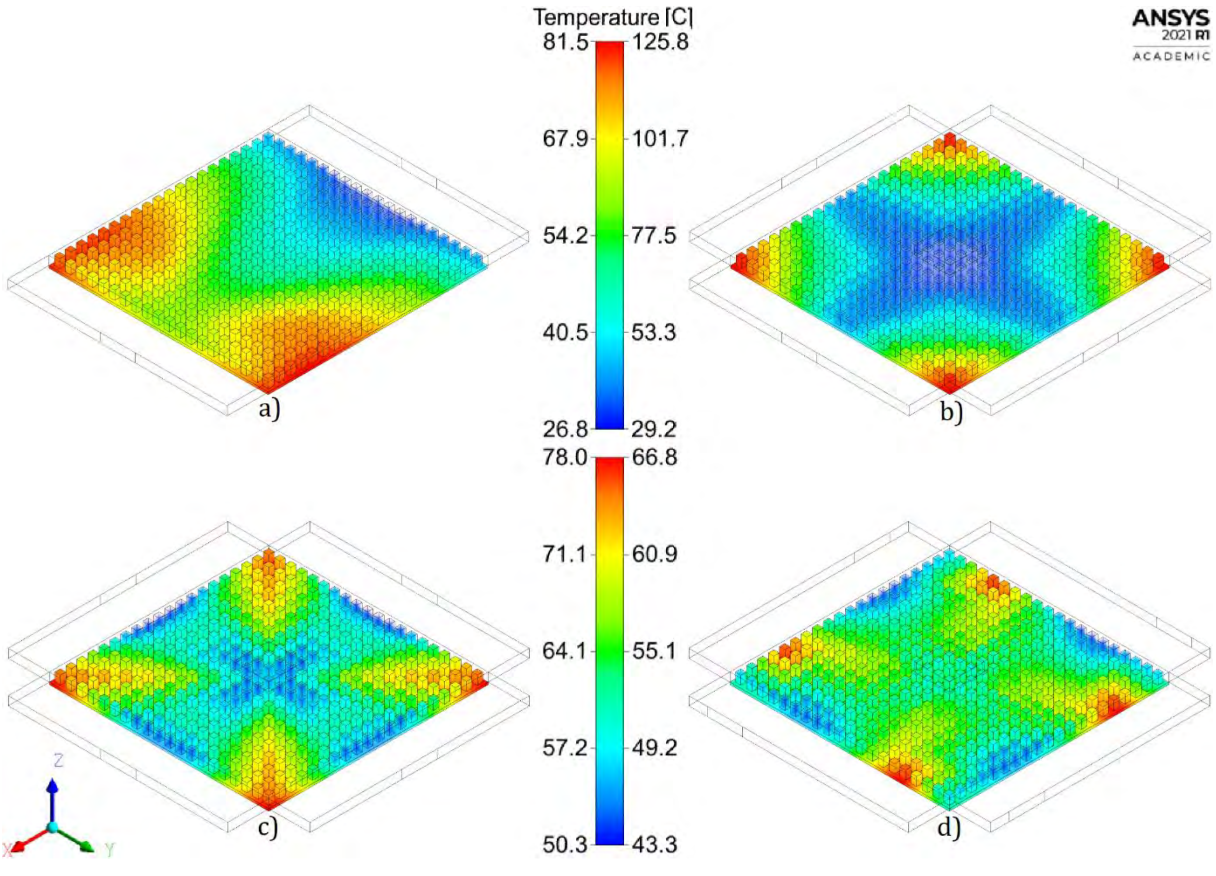

Figure 7: Temperature field of pin fins (solid domain) - local scale: a) Case 0; b) Case 1'; c) Case 2'; d) Case 3'

5. CONCLUSIONS

A detailed numerical investigation of novel MPFHS designs was performed to investigate their thermal performance and compare them with the conventional MPFHS design based on the 1 inlet and 1 outlet configuration. The novel designs are based on the 4 side manifolds instead of 2, as for the conventional case, and 1 manifold on the top of the heat sink. As a result, a flow can be realized in more ways than conventional design. There are 3 types of novel designs tested, namely 1 inlet channel on the top manifold and 4 outlet channels on the side manifolds (1in4out), 4 inlet channels on the side manifolds and 1 outlet channel on the top manifold (4in1out), and 4 inlet channels on the side manifolds with vortex configuration and 1 outlet channel on the top manifold (4in1out-vortex). The vortex configuration design showed very promising results so the study on side manifolds channels' position has been prepared to get the best thermohydraulic performance of the MPFHS.

The constant mass flow rate for the entire heat sink assumption has been taken into account. The results prove that the multiple inlet design with a vortex generator can be considered the best one compared to the conventional design.

Some novel designs show the reduced maximum temperature of the heat sink base referred to the conventional case, namely 21.1% and 4.3% for 4in1out-vortex (optimized) and 4in1out cases respectively, while the 1in4out case is characterized by 54.4% temperature increase. Moreover, the mean absolute temperature difference for MPFHS surface can be reduced up to 61.3% and 49.3% by utilizing 4in1out-vortex and 4in1out designs respectively which means that multiple inlet designs are characterized by more uniform temperature distribution. On the other hand, the 1in4out case causes the increase in mean absolute temperature difference by 76.3%. Also, the thermal resistance is smaller for multiple inlet designs, namely 23.5% and 5.9% for 4in1out-vortex and 4in1out cases respectively. The thermal resistance is increased for 1in4out case by 64.7%. The Nusselt numbers in the novel designs have not been improved due to the lower Reynolds number in pin fins compared to the conventional case. However, the overall thermal performance factor has been improved because of the reduced pressure drop for the novel designs. The Nusselt number is equal to 35.5, 35.3, 29.6, and 29.2 for conventional, 4in1out-vortex (optimized), 4in1out, and 1in4out cases respectively, while the total pressure drop in MPFHS of 8.5 kPa, 3.4 kPa, 3.2 kPa, and 3.1 kPa for conventional, 4in1out-vortex, 4in1out, and 1in4out cases respectively can be observed. Thereby, the overall thermal performance factor is equal to 1.34, 1.16, and 1.15 for 4in1out-vortex, 4in1out, and 1in4out cases respectively when the conventional case is treated as a baseline.

NOMENCLATURE

A	Heat exchange area (m^2)	Cp	Specific heat ($J \times kg^{-1} \times K^{-1}$)
Dh	Hydraulic diameter (m)	F	Tested parameter
G	Mass flux ($kg \times m^{-2} \times s^{-1}$))	k	Thermal conductivity ($W \times m^{-2} \times K^{-1}$)
$\dot{m}$	Mass flow rate ($kg \times s^{-1}$)	Nu	Nusselt number
p	Pressure (Pa)	q	Heat flux ($W \times m^{-2}$)
R	Thermal resistance ($K \times W^{-1}$)	Re	Reynolds number
T	Temperature (K)	V	Velocity ($m \times s^{-1}$)
δ	Mean average temp. difference (K)	Δp	Pressure drop (Pa)
η	Overall thermal performance factor	μ	Dynamic viscosity ($Pa \times s$)
ρ	Density ($kg \times m^{-3}$)		

REFERENCES

Cactus Technologies, Commercial and Industrial-Grade Products White Paper CTWP011, (2021).

D.B. Tuckerman, R.F.W. Pease, High-performance heat sinking for VLSI, IEEE Electron Device Lett. 2 (1981) 126–129.

I. Mudawar, Two-phase microchannel heat sinks : theory, applications, and limitations, J. Electron. Packag. 133 (2011) 041002(1)-041002(31). https://doi.org/10.1115/1.4005300.

S.T. Kadam, R. Kumar, Twenty first century cooling solution: Microchannel heat sinks, Int. J. Therm. Sci. 85 (2014) 73–92. https://doi.org/10.1016/j.ijthermalsci.2014.06.013.

M. Xu, H. Lu, L. Gong, J.C. Chai, X. Duan, Parametric numerical study of the flow and heat transfer in microchannel with dimples, Int. Commun. Heat Mass Transf. 76 (2016) 348–357. https://doi.org/10.1016/j.icheatmasstransfer.2016.06.002.

G. Wang, D. Niu, F. Xie, Y. Wang, X. Zhao, G. Ding, Experimental and numerical investigation of a microchannel heat sink (MCHS) with micro-scale ribs and grooves for chip cooling, Appl. Therm. Eng. 85 (2015) 61–70. https://doi.org/10.1016/j.applthermaleng.2015.04.009.

H. Shokouhmand, M. Aghvami, M.J. Afshin, Pressure drop and heat transfer of fully developed, laminar flow in rough, rectangular microchannels, in: ASME 2008 6th Int. Conf. Nanochannels, Microchannels, Minichannels, 2009: pp. 153–157.

L. Gong, K. Kota, W. Tao, Y. Joshi, Parametric numerical study of flow and heat transfer in microchannels with wavy walls, J. Heat Transfer. 133 (2011) 1–10. https://doi.org/10.1115/1.4003284.

H.A. Mohammed, P. Gunnasegaran, N.H. Shuaib, Influence of channel shape on the thermal and hydraulic performance of microchannel heat sink, Int. Commun. Heat Mass Transf. 38 (2011) 474–480. https://doi.org/10.1016/j.icheatmasstransfer.2010.12.031.

L. Chai, G. Xia, L. Wang, M. Zhou, Z. Cui, Heat transfer enhancement in microchannel heat sinks with periodic expansion–constriction cross-sections, Int. J. Heat Mass Transf. 62 (2013) 741–751. https://doi.org/10.1016/j.ijheatmasstransfer.2013.03.045.

Y.J. Lee, P.S. Lee, S.K. Chou, Numerical study of fluid flow and heat transfer in the enhanced microchannel with oblique fins, J. Heat Transfer. 135 (2013) 041901(1)-041901(10). https://doi.org/10.1115/1.4023029.

I.A. Ghani, N.A.C. Sidik, R. Mamat, G. Najafi, T.L. Ken, Y. Asako, Heat transfer enhancement in microchannel heat sink using hybrid technique of ribs and secondary channels, Int. J. Heat Mass Transf. 114 (2017) 640–655. https://doi.org/10.1016/j.ijheatmasstransfer.2017.06.103.

T. Hung, W. Yan, W. Li, Analysis of heat transfer characteristics of double-layered microchannel heat sink, Int. J. Heat Mass Transf. 55 (2012) 3090–3099. https://doi.org/10.1016/j.ijheatmasstransfer.2012.02.038.

S.P. Jang, S.U.S. Choi, Cooling performance of a microchannel heat sink with nanofluids, Appl. Therm. Eng. 26 (2006) 2457–2463. https://doi.org/10.1016/j.applthermaleng.2006.02.036.

C.J. Ho, L.C. Wei, Z.W. Li, An experimental investigation of forced convective cooling performance of a microchannel heat sink with Al2O3/water nanofluid, Appl. Therm. Eng. 30 (2010) 96–103. https://doi.org/10.1016/j.applthermaleng.2009.07.003.

T. Hung, W. Yan, X. Wang, C. Chang, Heat transfer enhancement in microchannel heat sinks using nanofluids, Int. J. Heat Mass Transf. 55 (2012b) 2559–2570. https://doi.org/10.1016/j.ijheatmasstransfer.2012.01.004.

V. Yadav, K. Baghel, R. Kumar, S.T. Kadam, Numerical investigation of heat transfer in extended surface microchannels, Int. J. Heat Mass Transf. 93 (2016) 612–622. https://doi.org/10.1016/j.ijheatmasstransfer.2015.10.023.

Y. Peles, A. Kosar, C. Mishra, C. Kuo, B. Schneider, Forced convective heat transfer across a pin fin micro heat sink, Int. J. Heat Mass Transf. 48 (2005) 3615–3627. https://doi.org/10.1016/j.ijheatmasstransfer.2005.03.017.

W. Qu, A. Siu-ho, Liquid single-phase flow in an array of micro-pin-fins — Part I : Heat transfer characteristics, J. Heat Transfer. 130 (2008) 122402(1)-122402(11). https://doi.org/10.1115/1.2970080.

C.A. Rubio-jimenez, S.G. Kandlikar, A. Hernandez-guerrero, Numerical analysis of novel micro pin fin heat sink with variable fin density, IEEE Trans. Components Packag. Manuf. Technol. 2 (2012) 825–833.

P. Dąbrowski, Thermohydraulic maldistribution reduction in mini heat exchangers, Appl. Therm. Eng. 173 (2020). https://doi.org/10.1016/j.applthermaleng.2020.115271.

R. Chein, J. Chen, Numerical study of the inlet/outlet arrangement effect on microchannel heat sink performance, Int. J. Therm. Sci. 48 (2009) 1627–1638. https://doi.org/10.1016/j.ijthermalsci.2008.12.019.

S.S. Sehgal, K. Murugesan, S.K. Mohapatra, Experimental investigation of the effect of flow arrangements on the performance of a micro-channel heat sink, Exp. Heat Transf. 24 (2011) 215–233. https://doi.org/10.1080/08916152.2010.523808.

M.S. V, A. Pattamatta, S.K. Das, Investigation on Flow Maldistribution in Parallel Microchannel Systems for Integrated Microelectronic Device Cooling, 4 (2014) 438–450.

G.D. Xia, J. Jiang, J. Wang, Y.L. Zhai, D.D. Ma, Effects of different geometric structures on fluid flow and heat transfer performance in microchannel heat sinks, Int. J. Heat Mass Transf. 80 (2015) 439–447. https://doi.org/10.1016/j.ijheatmasstransfer.2014.08.095.

V. Yadav, R. Kumar, A. Narain, Mitigation of flow maldistribution in parallel microchannel heat sink, IEEE Trans. Components, Packag. Manuf. Technol. 9 (2019) 247–261. https://doi.org/10.1109/TCPMT.2018.2851543.

R. Kumar, G. Singh, D. Mikielewicz, A new approach for the mitigating of flow maldistribution in parallel microchannel heat sink, J. Heat Transfer. 140 (2018) 072401–072410. https://doi.org/10.1115/1.4038830.

R. Kumar, R. Abiev, G. Ribatski, S. Abdullah, M. Vasilev, New Approach of Triumphing Temperature Nonuniformity and Heat Transfer Performance Augmentation in Micro Pin Fin Heat Sinks, J. Heat Transfer. 142 (2020) 602501(1)-602501(12). https://doi.org/10.1115/1.4046535.

X. Fang, Y. Xu, Z. Zhou, New correlations of single-phase friction factor for turbulent pipe flow and evaluation of existing single-phase friction factor correlations, Nucl. Eng. Des. 241 (2011) 897–902. https://doi.org/10.1016/j.nucengdes.2010.12.019.

Y.A. Çengel, A.J. Ghajar, Heat and Mass Transfer Fundamentals & Applications., Fifth Edit, McGraw-Hill Education, 2015.

T. Pham-Gia, T.L. Hung, The mean and median absolute deviations, Math. Comput. Model. 34 (2001) 921–936. https://doi.org/10.1016/S0895-7177(01)00109-1.

H. Wang, R.-Z. Wang, Q. Wu, C. Wang, A Universal High-Efficiency Cooling Structure for High-Power Integrated Circuits, SSRN Electron. J. (2022) 118849. https://doi.org/10.2139/ssrn.4049606.

Z. He, Y. Yan, Z. Zhang, Thermal management and temperature uniformity enhancement of electronic devices by micro heat sinks: A review, Energy. (2020) 119223. https://doi.org/10.1016/j.energy.2020.119223.

M.E. Polat, F. Ulger, S. Cadirci, Multi-objective optimization and performance assessment of microchannel heat sinks with micro pin-fins, Int. J. Therm. Sci. 174 (2022) 107432. https://doi.org/10.1016/j.ijthermalsci.2021.107432.

Y.A. Cengel, Thermodynamics : An Engineering Approach INTRODUCTION AND BASIC CONCEPTS, 8th Editio (2015) 1–59.